J|A|C|S
ARTICLES
Published on Web 09/11/2004

Cycloalkene Ozonolysis: Collisionally Mediated Mechanistic Branching

Bao Chuong, Jieyuan Zhang, and Neil M. Donahue*

Contribution from the Departments of Chemistry and Chemical Engineering, Carnegie Mellon University, Pittsburgh, Pennsylvania 15213

Received March 12, 2004; E-mail: nmd@andrew.cmu.edu

Abstract: Master equation calculations on a computational potential energy surface reveal that collisional stabilization at atmospheric pressure becomes important in the gas-phase ozonolysis of endocyclic alkenes for a carbon number between 8 and 15. Because the reaction products from endocyclic ozonolysis are tethered, this system is ideal for consideration of collisional energy transfer, as chemical activation is confined to a single reaction product. Collisional stabilization of the Criegee intermediate precedes collisional stabilization of the primary ozonide by roughly an order of magnitude in pressure. The stabilization of the Criegee intermediate leads to a dramatic transformation in the dominant oxidation pathway from a radical-forming process at low carbon number to a secondary ozonide-forming process at high carbon number. Secondary ozonide formation is important even for syn-isomer Criegee intermediates, contrary to previous speculation. We use substituted cyclohexenes as analogues for atmospherically important mono- and sesquiterpenes, which are major precursors for secondary organic aerosol formation in the atmosphere. Combining these calculations with literature experimental data, we conclude that the transformation from chemically activated to collisionally stabilized behavior most probably occurs between the mono- and sesquiterpenes, thus causing dramatically different atmospheric behavior.

Introduction

There is considerable interest in the mechanism of the gas-phase oxidation of alkenes by ozone. Annual global emissions of biogenic hydrocarbons greatly exceed those of anthropogenic hydrocarbons.[1] Biogenic emissions are dominated by isoprene, with substantial contributions from mono- and sesquiterpenes. Furthermore, modeling calculations have shown that ozone−alkene reactions can be a significant source of HO_x radicals, which are important atmospheric oxidants. This can be the leading HO_x source in urban and rural environments with sufficient alkene emissions,[2,3] in the nighttime,[4] and in indoor environments.[5] Ozone−alkene reactions can also lead to the production of secondary organic aerosol,[6−12] which can affect human health, climate, and visibility. Terpene ozonolysis is a major, perhaps dominant, source of secondary organic aerosol.[13,14]

Although the mechanism of the ozone−alkene reactions is not completely clear, the initial steps are generally believed to proceed via the Criegee mechanism[15] as shown in Scheme 1. The consensus description of this mechanism combines observational and computational evidence in the following sequence: ozone adds to the double bond in a concerted [2 + 3] cycloaddition to produce a vibrationally excited primary ozonide (POZ), which then quickly decomposes to yield an excited carbonyl oxide [Criegee intermediate (CI)] and a carbonyl compound. The excited CI may either undergo further unimolecular reactions or be collisionally stabilized. The particular unimolecular reaction pathway that is available to the CI will depend on its conformation. The syn carbonyl oxide (terminal oxygen facing an R group) leads to OH radicals with high efficiency after a 1,4-hydrogen shift to form a vinyl hydroperoxide intermediate, which then dissociates to form OH and a conjugated radical, whose likely fate is reaction with O_2 and NO and decomposition to produce a C_5-dialdehyde, CO, and HO_2.[16] The anti carbonyl oxide (terminal oxygen facing a hydrogen atom) leads instead to a dioxirane via ring closure,

(1) Guenther, A.; Hewitt, C. N.; Erickson, D.; Fall, R.; Geron, C.; Graedel, T.; Harley, P.; Klinger, L.; Lerdau, M.; McKay, W. A.; Pierce, T.; Scholes, B.; Steinbrecher, R.; Tallamraju, R.; Taylor, J.; Zimmerman, P. *J. Geophys. Res.* **1995**, *100*, 8873.
(2) Paulson, S. E.; Orlando, J. J.*Geophys. Res. Lett.* **1996**, *23*, 3727.
(3) Ariya, P. A.; Sander, R.; Crutzen, P. J. *J. Geophys. Res.* **2000**, *105*, 17721.
(4) Bey, I.; Aumont, B.; Toupance G. *Geophys. Res. Lett.* **1997**, *24*, 1067.
(5) Weschler, C. J.; Shields, H. C. *Environ. Sci. Technol.* **1996**, *30*, 3250.
(6) Hatakeyama, S.; Tanonaka, T.; Weng, J.; Bandow, H.; Takagi, H.; Akimoto, H. *Environ. Sci. Technol.* **1985**, *19*, 935.
(7) Yokouchi, Y.; Ambe, Y. *Atmos. Environ.* **1985**, *19*, 1271.
(8) Hatakeyama, S.; Ohno, M.; Weng, J.-H.; Takagi, H.; Akimoto, H. *Environ. Sci. Technol.* **1987**, *21*, 52.
(9) Hatakeyama, S.; Izumi, K.; Fukuyama, T.; Akimoto, H. *J. Geophys. Res.* **1989**, *94*, 13013.
(10) Hoffman, T.; Odum, J. R.; Bowman, F.; Collins, D.; Klockow, D.; Flagan, R. C.; Seinfeld, J. H. *J. Atmos. Chem.* **1997**, *26*, 189.
(11) Kalberer, M.; Yu, J.; Cocker, D. R.; Flagan, R. C.; Seinfeld, J. H. *Environ. Sci. Technol.* **2000**, *34*, 4894.
(12) Ziemann, P. J. *J. Phys. Chem. A* **2002**, *106*, 4390.
(13) Pandis, S.; Paulson, S.; Seinfeld, J.; Flagan, R. *Atmos. Environ.* **1992**, *26A*, 2266.
(14) Yu, J.; Cocker, D. R., III; Griffin, R. J.; Flagan, R.; Seinfeld, J. H. *J. Atmos. Chem.* **1999**, *34*, 207.
(15) Criegee, R. *Angew. Chem., Int. Ed.* **1975**, *14*, 745−751.
(16) Salisbury, G.; Rickard, A. R.; Monks, P. S.; Allan, B. J.; Bauguitte, S.; Penkett, S. A.; Carslaw, N.; Lewis, A. C.; Creasey, D. J.; Heard, D. E.; Jacobs, P. J.; Lee, J. D. *J. Geophys. Res.* **2001**, *106*, 12669.

Scheme 1. Mechanism for Ozonolysis of *trans*-2-Butene

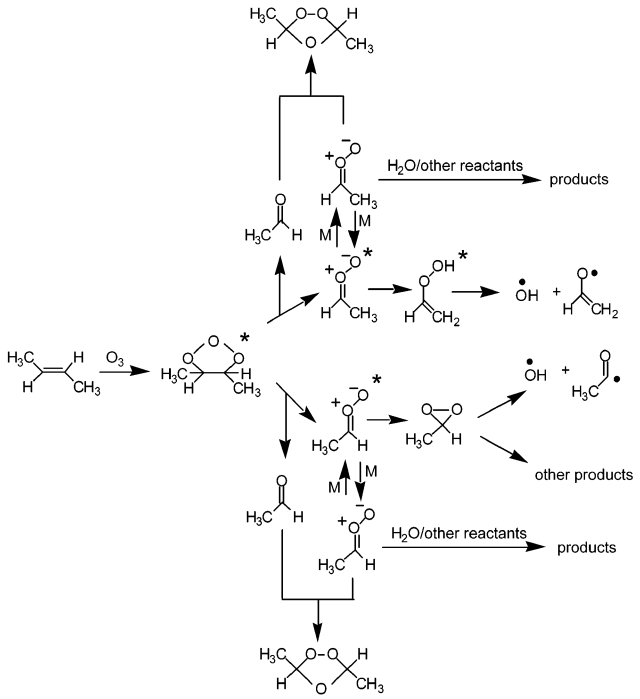

which then may undergo ring cleavage and isomerization to produce a "hot" organic acid or ester, though this is a subject of controversy.[17,18] Subsequent dissociation of the "hot" organic acid can lead to the production of H, R, and OH radicals. Interconversion between the syn and anti isomers is not likely to occur because of the large energy barrier for interconversion.[19]

Besides undergoing unimolecular reaction, the excited CI may be collisionally stabilized as shown in Scheme 1. In fact, all intermediates along the reaction coordinate will suffer collisions, with the longest-lived intermediate being the most susceptible to stabilization. This appears to be the CI. Once stabilized, the CI may react with the carbonyl compound (produced from the cycloreversion of the POZ) to form a secondary ozonide (SOZ). At typical ambient concentrations in the gas phase this is unlikely, as the bimolecular products will separate; however, the stabilized Criegee intermediate (SCI) may participate in bimolecular reactions with water,[20−23] SO_2,[24−26] organic acids,[27] carbonyl species,[28] NO_x,[29] and hexafluoroacetone.[30]

A major area of uncertainty in the ozone−alkene reaction mechanism concerns the competition between collisional stabilization and unimolecular reaction of the energy-rich reactive intermediates, including the CI. Although pressure-dependent product studies should clarify this uncertainty, these studies have offered conflicting data. A recent radical-tracer study in which OH yield from the ozonolysis of 1-butene, *trans*-2-butene, 2,3-dimethyl-2-butene, cyclopentene, and *trans*-3-hexene was measured from 20 to 760 Torr suggests that there is no pressure dependence.[31] In the same study, a pressure dependence was observed, however, for the ozonolysis of ethene and propene, and the authors propose that the production of a hydroperoxide, which can lead to OH formation, can compete with the production of the CI.[31] In addition, radical-tracer studies of OH yields from ozone reaction with cycloalkenes[32] at 1 atm suggest that collisional stabilization is not important since OH yields did not decrease with increasing alkene size. Although Paulson et al.[33] found that OH yields decrease with increasing size of terminal alkenes, they attributed this to an evolving syn−anti ratio in the CI. Along with the authors of other studies, they conclude that OH yields can be better predicted using structure−activity relationships (SARs) based on the level of substitution of the CI, rather than substituent size and available vibrational energy.[33−35] Because there appears to be no dependence of collisional stabilization on size, this suggests there is no competition between collisional stabilization and unimolecular reaction. These results are in contrast to those from a number of experimental and theoretical studies. Direct pressure-dependent studies of OH yields from ozone−alkene reactions using the high-pressure flow system (HPFS) with laser-induced fluorescence (LIF) detection of OH indicated a pressure dependence for substituted alkenes.[36] Furthermore, a pressure dependence was observed for the SCI from the oxidation of SO_2 in the ozone + *trans*-2-butene reaction.[26] In addition, time-dependent master equation calculations predict a pressure dependence for the ozonolysis of a number of alkenes.[37,38]

The experimental results of Kroll et al.[36] suggest that at atmospheric pressure, OH production is a result of the thermal decomposition of stabilized Criegee intermediates. This has important atmospheric implications. Because stabilized Criegee intermediates are known to undergo bimolecular reactions as discussed above, they could compete with the unimolecular channel if these bimolecular reactions are fast.[39] Therefore, it is important to resolve the uncertainty concerning competition between collisional stabilization and unimolecular reaction in the ozone−alkene reaction mechanism.

Several factors may cloud this discussion. First, while collisional stabilization may be unimportant for some range of carbon numbers, it almost certainly becomes important at *some* carbon number. Second, it is not necessary that stabilization alter the mechanism in any way, though it may; bimolecular reactions *may* compete with unimolecular reactions for the

(17) Kroll, J. H.; Donahue, N. M.; Cee, V. J.; Demerjian, K. L.; Anderson, J. G. *J. Am. Chem. Soc.* **2002**, *124*, 8518.
(18) Kuwata, K. T.; Templeton, K. L.; Hasson, A. S. *J. Phys. Chem. A* **2003**, *107*, 11525.
(19) Anglada, J. M.; Bofille, J. M.; Olivella, S.; Sole, A. *J. Am. Chem. Soc.* **1996**, *118*, 4636.
(20) Hatakeyama, S.; Lai, H.; Gao, S.; Murano, K. *Chem. Lett.* **1993**, 1287.
(21) Hasson, A. S.; Orzechowska, G.; Paulson, S. E. *J. Geophys. Res.* **2001**, *106*, 34131.
(22) Hasson, A. S.; Ho, A. W.; Kuwata, K. T.; Paulson, S. E. *J. Geophys. Res.* **2001**, *106*, 34143.
(23) Baker, J.; Aschmann, S. M.; Arey, J.; Atkinson, R. *Int. J. Chem. Kinet.* **2002**, *34*, 73.
(24) Cox, R. A.; Penkett, S. A. *Nature* **1971**, *230*, 321.
(25) Cox, R. A.; Penkett, S. A. *J. Chem. Soc., Faraday Trans. 1* **1972**, *68*, 1735.
(26) Hatakeyama, S.; Kobayashi, H.; Akimoto, H. *J. Phys. Chem.* **1984**, *88*, 4736.
(27) Neeb, P.; Horie, O.; Moortgat, G. K. *Int. J. Chem. Kinet.* **1996**, *28*, 721.
(28) Neeb, P.; Horie, O.; Moortgat, G. K. *Tetrahedron Lett.* **1996**, *37*, 9297.
(29) Atkinson, R.; Lloyd, A. C. *J. Phys. Chem. Ref. Data* **1984**, *13*, 315.
(30) Horie, O.; Schafer, C.; Moortgat, G. K. *Int. J. Chem. Kinet.* **1999**, *31*, 261.
(31) Fenske, J. D.; Hasson, A. S.; Paulson, S. E.; Kuwata, K. T.; Ho, A. W.; Houk, K. N. *J. Phys. Chem. A* **2000**, *104*, 7821.
(32) Fenske, J. D.; Kuwata, K. T.; Houk, K. N.; Paulson, S. E. *J. Phys. Chem. A* **2000**, *104*, 7246.
(33) Paulson, S. E.; Chung, M. Y.; Hasson, A. S. *J. Phys. Chem. A* **1999**, *103*, 8125.
(34) Atkinson, R.; Aschmann, S. M. *Environ. Sci. Technol.* **1993**, *27*, 1357.
(35) Rickard, A. R.; Johnson, D.; McGill, C. D.; Marston, G. *J. Phys. Chem. A* **1999**, *103*, 7656.
(36) Kroll, J. H.; Clarke, J. S.; Donahue, N. M.; Anderson, J. G.; Demerjian, K. L. *J. Phys. Chem. A* **2001**, *105*, 1554.
(37) Olzmann, M.; Kraka, E.; Cremer, D.; Gutbrod, R.; Andersson, S. *J. Phys. Chem. A* **1997**, *101*, 9421.
(38) Kroll, J. H.; Sahay, S. R.; Anderson, J. G.; Demerjian, K. L.; Donahue, N. M. *J. Phys. Chem. A* **2001**, *105*, 4446.
(39) Johnson, D.; Lewin, A. G.; Marston, G. *J. Phys. Chem. A* **2001**, *105*, 2933.

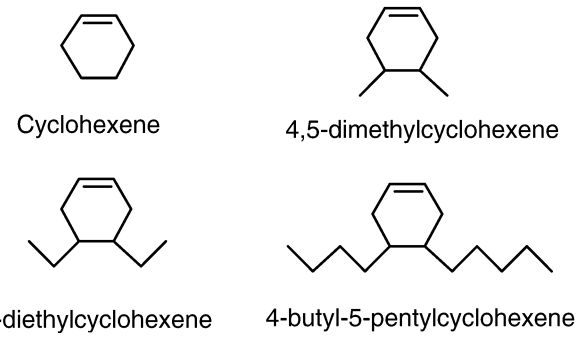

Figure 1. Chemical structures of the series of cyclohexenes studied in this work.

stabilized intermediate, and unimolecular branching *may* change with energy. Finally, it must always be remembered that collisional stabilization may in fact occur in a number of different isomers or wells; while there is as yet no compelling evidence of this, it provides a potential resolution to seemingly conflicting experimental data.

An additional source of uncertainty is that the origin of SCIs is unclear. While observations of reaction products such as secondary organic aerosols[10,14,40−44] and α-hydroperoxides[21,22] clearly suggest that SCIs are being formed in many cases, these observations are confined to linear alkenes, where the excess reaction energy will be distributed among two reaction products (CI + carbonyl product) as well as external modes (translation and rotation of the products). Consequently, "stabilized" can indicate either intermediates that are formed with relatively low internal energy—and thus easily thermalized—or those that undergo extensive collisional stabilization.

We have used RRKM/master equation calculations to determine the fate of the energy-rich primary ozonide and Criegee intermediates in the ozonolysis of a series of cyclohexenes (cyclohexene, 4,5-dimethylcyclohexene, 4,5-diethylcyclohexene, and 4-butyl-5-pentylcyclohexene) as shown in Figure 1. We chose to study cyclohexenes because they are analogues for the important biogenic monoterpene and sesquiterpene hydrocarbons, containing the essential properties of the more complicated terpene systems. Altough monoterpenes and sesquiterpenes have fewer hydrogens than the alkyl-substituted C_{10} and C_{15} cyclohexenes under consideration here, this should have minimal effect on the results.

Endocyclic alkenes, such as cyclohexene, are fundamentally interesting because the carbonyl and CI ozonolysis products are tethered and thus form a single, disubstituted product (see Scheme 2). This tethering has two consequences: it removes the significant complication of energy distribution between the bimolecular fragments intrinsic to acyclic alkenes, and it holds the carbonyl group close to the CI. The thermal energy distribution of the initial reaction products is vastly less than the reaction exothermicity, so the product energy distribution approaches a delta function.

Scheme 2. Mechanism for Ozonolysis of Cylohexene

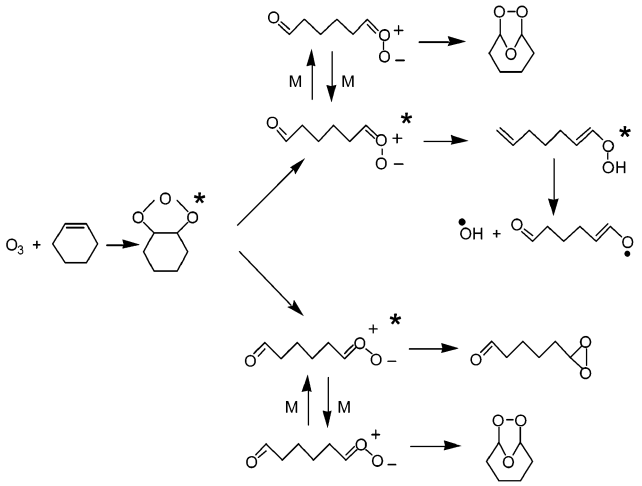

Finally, unlike the case of the acyclic alkenes, SOZs can be produced through cyclization of the CI as a result of the interaction between the Criegee moiety and the carbonyl group (see Scheme 2). This intramolecular reaction is known to occur in the ozonolysis of cycloalkenes.[45] The production of these secondary ozonides may only be likely, however, if the Criegee intermediates have been collisionally stabilized, and this is one aspect of the central hypothesis (described below) that is being explored in this research. It has also been proposed that this intramolecular SOZ formation occurs only out of the anti-CI,[46] as the syn-CI appears to be considerably strained in a transition state to SOZ. Regardless, stabilization should depend on carbon number. Consequently, it is possible that the ozonolysis mechanism has a significant size dependence, caused by a relationship between size and collisional stabilization. This mechanistic shift could have dramatic consequences, ranging from formation of radical products—including OH—at low carbon numbers or low pressure, to stoichiometric formation of SOZ—and presumably organic aerosol—at high carbon numbers or high pressure. The crossover may be relatively sudden, occurring over a narrow range of carbon numbers.

Understanding the role of collisional stabilization is important for reasons already presented above and because current models for secondary organic aerosol formation[47] and the equilibrium between atmospheric aerosol condensation and evaporation processes[48] do not consider collisional stabilization, the potential for secondary association reactions, or the potential for irreversible adsorption of low-vapor-pressure stabilized intermediates onto existing aerosols. For example, SOZ formed from ozonolysis may decompose once it condenses. While many products produced from the gas-phase oxidation of monoterpenes and sesquiterpenes (i.e., pinic acid, pinonic acid, and nopinone) can lead to the formation of SOA or incorporation into SOA,[40,44,49] it is the distribution of vapor pressures among the products that ultimately governs SOA yields. This depends on the mechanistic details.

(40) Jang, M.; Kamens, R. M. *Atmos. Environ.* **1999**, *33*, 459.
(41) Kamens, R. M.; Jang, M.; Leach, B. K.; Chien, C. *Environ. Sci. Technol.* **1999**, *33*, 1430.
(42) Yu, J.; Cocker, D. R., III; Griffin, R. J.; Flagan, R. C.; Seinfeld, J. H. *Geophys. Res. Lett.* **1999**, *26*, 1145.
(43) Koch, S.; Winterhalter, R.; Uherek, E.; Kolloff, A.; Neeb, P.; Moortgat, G. K. *Atmos. Environ.* **2000**, *34*, 4031.
(44) Winterhalter, R.; Neeb, P.; Grossmann, D.; Kolloff, A.; Horie, O.; Moortgat, G. *J. Atmos. Chem.* **2000**, *35*, 165.
(45) Bailey, P. S. *Ozonation in Organic Chemistry, Volume I, Olefinic Compounds*; Academic Press: New York, 1978.
(46) Aschmann, S. M.; Tuazon, E. C.; Arey, J.; Atkinson, R. *J. Phys. Chem. A* **2003**, *107*, 2247.
(47) Griffin, R. J.; Nguyen, K.; Dabdub, D.; Seinfeld, J. H. *J. Atmos. Chem.* **2003**, *44*, 171.
(48) Gaydos, T. M.; Koo, B.; Pandis, S. N.; Chock, D. P. *Atmos. Environ.* **2003**, *37*, 3303.
(49) Jaoui, M.; Kamens, R. M. *J. Atmos. Chem.* **2003**, *46*, 29.

Our objective is to determine the degree of collisional stabilization of ozonolysis intermediates derived from cyclohexene and alkyl-substituted cyclohexenes, the dependence of stabilization on size and pressure, and the origin of the SCI. Our central hypothesis is this: at some critical size (carbon number), ozonolysis of endocyclic alkenes switches from a pathway directed toward ultimate formation of OH radicals, with high efficiency, to a pathway routed through the SOZ, presumably devoid of OH radical production but potentially very efficient at the formation of organic aerosols. This motivates a number of simplifying assumptions. First, we shall consider the anti and syn Criegee intermediates separately because simultaneous consideration of the relatively complicated issues presented here and the equally complicated question of the syn/anti branching ratio would obscure our primary objective. For clarity our discussion will focus on the syn pathway. The results (presented below) are similar for both pathways, the branching ratio for the syn pathway is ~60% in the O_3−cyclohexene reaction, and the syn pathway is somewhat more interesting because of its high potential OH yields. Second, we shall use a low-level potential energy surface (B3LYP/6-31G(d)) for the base cyclohexene system and treat substituent R groups far from the double bond for larger system by simply adding characteristic modes to our master equation calculations. Third, we shall not consider the ultimate fate of the various CI decomposition products, but rather assume that each pathway has a characteristic signature (for instance, formation of a vinyl hydroperoxide produces OH radicals with unit efficiency). Each of these areas awaits future consideration.

Quantum Chemical Calculations

Geometries, energies, and frequencies are calculated using density functional theory, employing Becke's three-parameter hybrid functional B3LYP and the 6-31G(d) basis set. These calculations are performed using the Gaussian98 program.[50] The calculated frequencies are scaled by the recommended factor of 0.9613.[51] While the density functional calculations are not as accurate as ab initio methods with a high degree of electron correlation, we feel that the accuracy is more than adequate for the current purpose, which is to examine the broad dependence of the target systems on carbon number. To that end, we have optimized only the O_3−cyclohexene system; our higher carbon number terpene analogues are nominally 4,5-disubstituted cyclohexenes, which we model simply by introducing additional frequencies (including hindered rotations) into our microcanonical RRKM rate constants.

Theoretical Methods

Because the master equation has been described in detail elsewhere,[38,52] only a brief description of it is given here. The master equation describes the time- and energy-dependent population $N(E,t)$ of an intermediate species subject to competition between collisional stabilization and reactions and is given by

$$\frac{dN}{dt} = rF - [\omega(\mathbf{I} - \mathbf{P}) + \sum K_i]N = rF - \mathbf{J}N \qquad (1)$$

where r is the overall rate of formation of the intermediate species, F the normalized vibrational flux distribution of the reactants, $\mathbf{P}$ the normalized energy transfer matrix, $\mathbf{I}$ the unit matrix, ω the collision frequency, and K_i a diagonal matrix of microcanonical rate constants for the ith channel. The solution to eq 1 has been solved and may be expressed as

$$N(t) = r\mathbf{U}\mathbf{L}\mathbf{U}^{-1}F \qquad (2)$$

where $\mathbf{U}$ is the corresponding eigenvector matrix of matrix $\mathbf{J}$, and $\mathbf{L}$ is a diagonal matrix with diagonal elements $L_i = (1 - \exp(-\lambda_i t))/\lambda_i$.

To use the master equation, the first step is to calculate the energy transfer matrix $\mathbf{P}$ for both downward and upward transitions. $\mathbf{P}_{ij}$, the probability that a molecule at energy j will transfer to energy i after a collision, is the energy transfer matrix for downward transitions and is given by

$$\mathbf{P}_{ij} \propto \left(\frac{\rho_j}{\rho_i}\right) \exp\left(\frac{-\Delta E}{\langle \Delta E \rangle_{\text{down}}}\right) \qquad (3)$$

where ρ_j is the density of states of the reactant at energy j, ρ_i the density of states of the reactant at energy i, and $\langle \Delta E \rangle_{\text{down}}$ the average energy lost per deactivating collision. $\langle \Delta E \rangle_{\text{down}}$ was set to 500 cm^{-1} for these calculations, and the effect of changing $\langle \Delta E \rangle_{\text{down}}$ on our calculations is addressed in the Supporting Information. $\mathbf{P}_{ji}$, the probability that a molecule at energy i will transfer to energy j after a collision, is the energy transfer matrix for upward transitions and is related to $\mathbf{P}_{ij}$ through detailed balance:

$$\frac{\mathbf{P}_{ji}}{\mathbf{P}_{ij}} = \left(\frac{\rho_j}{\rho_i}\right) \exp\left(\frac{-\Delta E}{kT}\right) \qquad (4)$$

where k is the Boltzmann constant. Equation 4 enforces a Boltzmann distribution in the absence of reactions. Because the intermediate species will not disappear in a collision, $\sum_i \mathbf{P}_{ij} = 1$.

On the basis of RRKM theory, the microcanonical rate constant k at energy E [$k(E)$] is calculated as follows (with E in units of cm^{-1}):

$$k(E) = \frac{cG(E - E_{\text{crit}})}{\rho(E)} \qquad (5)$$

where c is the speed of light, $G(E - E_{\text{crit}})$ the accumulated density of the transition state at energy $(E - E_{\text{crit}})$, E_{crit} the critical energy of the transition state, and $\rho(E)$ the density of state of the reactant at energy E. Rovibrational sums and

(50) Frisch, M. J.; Trucks, G. W.; Schlegel, H. B.; Scuseria, G. E.; Robb, M. A.; Cheeseman, J. R.; Zakrzewski, V. J.; Montgomery, J. A.; Strapmann, R. E.; Durant, J. C.; Dapprich, S.; Millam, J. M.; Daniels, A. D.; Kudin, K. N.; Strain, M. C.; Farkas, O.; Tomasi, J.; Barone, V.; Cossi, M.; Cammi, R.; Mannucci, B.; Pomelli, C.; Adamo, C.; Clifford, S.; Ochterski, J.; Petersson, G. A.; Ayala, P. Y.; Cui, Q.; Morokuma, K.; Malick, D. K.; Rabuck, A. D.; Raghavachari, K.; Foresman, J. B.; Cioslowski, J.; Ortiz, J. V.; Stefanov, B. B.; Liu, J.; Liashenko, A.; Piskorz, P.; Komaromi, I.; Gomperts, R.; Martin, R. L.; Fox, D. J.; Keith, T.; Al-Laham, M. A.; Peng, C. Y.; Nanayakkara, A.; Gonsalez, C.; Challacombe, M.; Gill, P. M. W.; Johnson, B.; Chen, W.; Wong, M. W.; Andres, J. L.; Gonzalez, C.; Head-Gordon, M.; Replogle, E. S.; Pople, J. A. *Gaussian 98*, Revision A, 6th ed.; Gaussian, Inc.: Pittsburgh, PA, 1998.
(51) Wong, M. W. *Chem. Phys. Lett.* **1996**, *256*, 391.
(52) Holbrook, K. A.; Pilling, M. J.; Robertson, S. H. *Unimolecular Reactions*; John Wiley & Sons: New York, 1996.

densities of states are calculated using Professor John Barker's DenSum program.[53]

For long alkyl chains, including the "unwound" CI and the side chains of the substituted cyclohexenes, we must consider multiple conformations. Our assumption here is that these conformations all have nearly the same energy (this is borne out by our computational results). Consequently, we model the hindered internal rotors associated with the conformational transitions with a modified version of the hindered rotor formulation in DenSum. We describe the hindered rotors with a limiting frequency, an isomerization barrier height, and two symmetry numbers—the number of minima in a full 2π rotation, and the formal symmetry number. In this case, with methyl-type rotations but no actual symmetry, we have three minima in 2π but a formal symmetry number of 1. In this way, we describe the density of states over a manifold of 243 indistinguishable conformations of the C_6 CI. This is a substantial simplification—for example, we make no effort to identify sterically impossible conformations—but it is adequate for our current purposes. These modifications have been incorporated into the current version of the DenSum program.[54]

We solve the master equation via matrix inversion, using a Matlab-based code developed at Carnegie Mellon University for the purpose. Following the lead of Multiwell,[53] we treat variable energy grain sizes in the matrix, with high resolution near transition-state energies and lower resolutions elsewhere. Grain resolution at the base of the wells is treated at high resolution if we wish to accurately model thermal dissociation rates; otherwise it is left at low resolution. One of the shortcomings of a matrix-based solution is that the matrix inversions become poorly conditioned as the Boltzmann term coupling the extreme energies in the matrix approaches some factor of the machine precision; this generates instabilities when the energy range is large or when the temperature is low. In our case, master equation calculations on the ozonolysis of cyclohexene, 4,5-dimethylcyclohexene, 4,5-diethylcyclohexene, and 4-butyl-5-pentylcyclohexene were performed at 400 K to avoid unstable inversions. The phenomena under consideration here are described by characteristic energies of 1000 cm^{-1} and more, and the chemical activation energy is nearly 30 000 cm^{-1}, so there will be minimal differences between 300 and 400 K calculations (we have verified this with calculations treating a reduced energy range). Finally, our system includes multiple wells, but they are connected as a cascade, with an effectively irreversible progression from one well to the next; we can thus treat the multiwell problem as a succession of single-well problems, with the output flux from one defining the input flux to the next, rather than a coupled multiwell calculation, which is much more demanding (scaling like N^2, where N is the number of wells). As we shall see, there is no back flux from the CI to the POZ, so we can model the system with a succession of single-well calculations, first the POZ, and then the CI.

Results and Discussion

The potential energy surface for the O_3−cyclohexene reaction is shown in Figure 2. The energies shown are the optimized, zero-point-corrected energies relative to the CI. The optimized geometries for each species, including the POZ, CI, and the vinyl hydroperoxide, are one of many conformations (e.g., 243 total conformations for the CI) given the large number of degrees of freedom of these molecules. Interconversion between the different conformations should not significantly affect the overall potential energy surface since the barriers are less than 4 kcal mol^{-1}. For example, the different conformations in the CI involve rotations of the carbon groups, which is approximately a 3 kcal mol^{-1} barrier, not enough to significantly affect master equation calculation results. The potential energy surface for the anti pathway is similar to that for the syn pathway. Though the TS energy for the anti-CI to dioxirane is 13.3 kcal mol^{-1}, slightly smaller than that for the syn-CI to vinyl hydroperoxide channel, this did not affect the conclusions of this work as discussed later. It should be noted that the B3LYP/6-31G(d) level of theory did not provide a reasonable energy for the O_3 + cyclohexene transition state, and the energy of 74.7 kcal mol^{-1} in Figure 2 was determined using statistical mechanics. Although the basis set used to determine the potential energy surface is slightly smaller than the 6-31G(d,p) used by Fenske et al.,[32] the difference should not affect the fundamental conclusions of this research. It should also be noted that we assume that the potential energy surfaces for the ozonolysis of all the alkyl-substituted cyclohexenes studied in this work are the same as that for cyclohexene. This assumption could be made because the alkyl substituents do not participate in the ozonolysis and subsequent reactions. The sole role of these alkyl substituents will be to store the chemical activation energy and thus lower the microcanonical rate constants.

Of particular interest is our finding that the syn SCI under consideration here can easily cyclize to form SOZ. The reaction is entropically disfavored—only one of the 243 conformers of the syn cyclohexene SCI can form the SOZ (though it is the most stable of those we have optimized), but the reaction proceeds over a very low barrier of 5.1 kcal mol^{-1}. This is in contrast to a recent experimental study proposing cyclization of the anti isomer as the only intramolecular pathway to form SOZ.[46] The transition state geometry is shown in Figure 3, with displacement vectors for the imaginary frequency clearly indicating the cyclization. Note as well that the Criegee moiety is clearly syn, and that the reactive motion is breaking the planarity of the CI in favor of the ring structure.

Figure 4 shows the microcanonical rate constants for the two different reaction pathways coming out of the POZ well in the O_3−cyclohexene reaction (i.e., cycloreversion to form the CI and re-formation of the reactants). We have considered only the concerted cycloreversion pathway, as computational studies of the nonconcerted (stepwise) pathway reveal a second barrier (for O−O bond cleavage) significantly higher than the initial C−C barrier (which itself is competitive with the concerted cycloreversion barrier).[55] At the available energy of ~26 000 cm^{-1}, cycloreversion to form the CI dominates and re-formation of reactants is completely negligible. Furthermore, collisional stabilization of the cyclohexene POZ is out of the question at 1 atm pressure, where the collision frequency, ω, is approximately 1×10^{10} s^{-1}. The energy of POZ formation (the O_3−cyclohexene TS energy) is approximately 27 000 cm^{-1}, and the microcanonical cycloreversion rate constant is also 1×10^{10}

(53) Barker, J. R. *Multiwell*, 1.3.3 ed.; University of Michigan: Ann Arbor, MI, 2003 (http://data.engin.umich.edu/multiwell/multi-distrib.htm).
(54) Barker, J. R. Personal communication, 2003.
(55) Anglada, J. M.; Crehuet, R.; Bofill, J. M. *Chem. Eur. J.* **1999**, *5*, 1809.

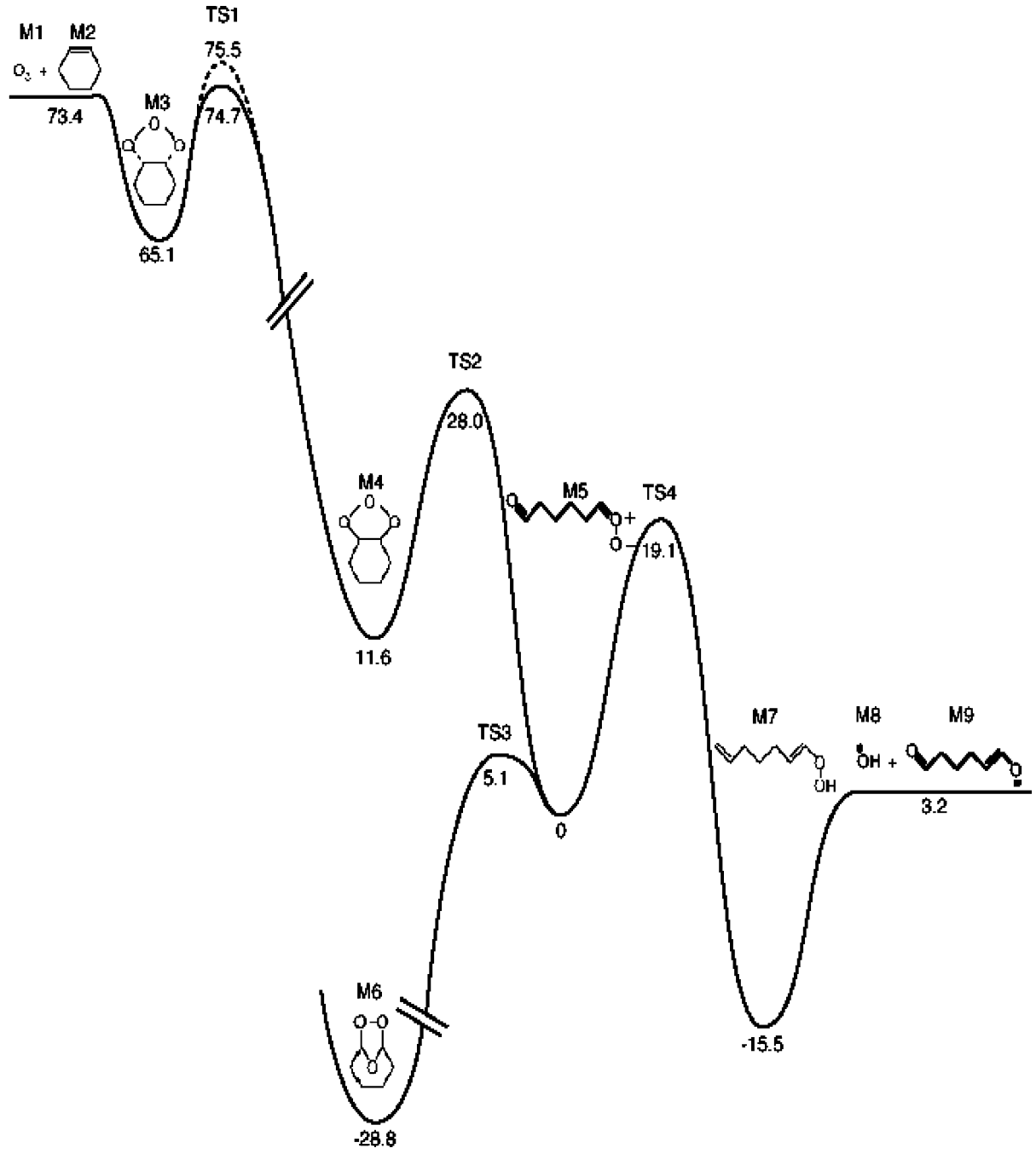

Figure 2. Zero-point-corrected potential energy surface for the O_3-cyclohexene reaction (syn pathway) calculated at the B3LYP/6-31G(d) level of theory. M3 is a van der Waals complex, and M4 is the POZ. Energies are in kcal mol^{-1} and are relative to the CI well. The only available experimental value for comparison is the O_3 + cyclohexene transition state (TS1). The dashed line with a maximum of 75.5 kcal mol^{-1} is the experimental activation energy reported by Treacy et al.[60]

s^{-1} at 27 000 cm^{-1}. Consequently, the POZ will decompose after an average of one collision, which will remove far less energy than necessary (perhaps 500 cm^{-1}). Similar results were also observed for the C_8-C_{15} alkyl-substituted cyclohexenes, with lower microcanonical rate constants due to the increased size.

The microcanonical rate constants for the different reaction pathways coming out of the syn-CI well (i.e., vinyl hydroperoxide pathway to produce OH, SOZ production, and reformation of the POZ) in the O_3-cyclohexene reaction are shown in Figure 5. At the available energy of ~26 000 cm^{-1}, production of vinyl hydroperoxide is the dominant pathway. At thermal energies, production of the SOZ is the dominant pathway. The total rate constant at high energies out of the syn-CI well is lower than the rate constant out of the POZ well by nearly an order of magnitude; consequently, as pressure or carbon number is increased, collisional stabilization will occur first in the syn-CI, then in the POZ. Any thermalized POZ, which will rapidly decompose to form syn-CI, will thus also lead to thermalized syn-CI. This in turn will yield SOZ, which will again certainly stabilize. Conversely, essentially all vinyl hydroperoxide production will include substantial chemical activation, with the following (presumably facile) bond fission occurring very rapidly thereafter.

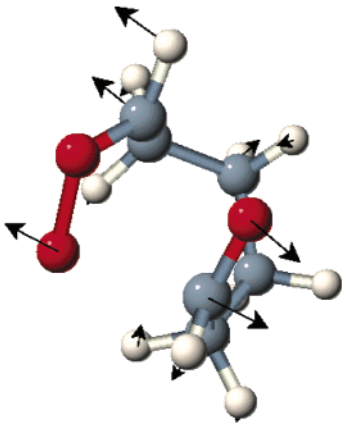

Figure 3. Transition state geometry for the SCI (M5)-to-SOZ (M6) intramolecular reaction (TS3). Arrows are the displacement vectors for the imaginary frequency, showing clearly that the syn carbonyl oxide moiety in the upper left leads to a secondary ozonide.

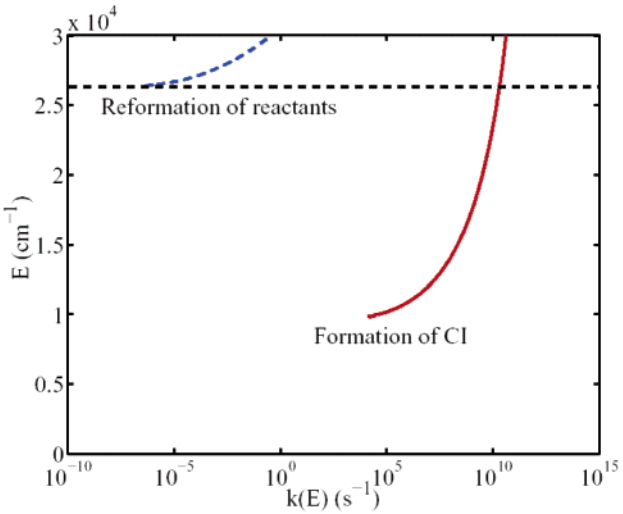

Figure 4. Microcanonical rate constants for the reaction pathways coming out of the POZ well (M4) in the O_3−cyclohexene reaction. Formation of the CI (M5 via TS2, solid red line) dominates over a return to reactants (M1 + M2 via TS1, dashed blue line) by 10 orders of magnitude. Note that energy in all microcanonical figures is plotted on the *y* axis, and all energies are plotted with respect to the zero in Figure 2. The available energy is approximately 26 000 cm^{-1}, near the top of the figure, and is designated by the horizontal black dashed line.

The effect of increased carbon number is more subtle for the CI than for the POZ. As the carbon number increases, the microcanonical rate constant curve for the OH pathway shifts to lower values, while that for the SOZ pathway does not shift significantly. The cause is the different barrier heights. The critical energy for vinyl hydroperoxide formation (and thus OH production) is a good fraction (1/4) of the available energy, while the critical energy for SOZ formation is less than 1/10 of the available energy. So far above both the barrier and the well, the SOZ formation channel is dominated by entropy—in this case the constraint of forming a bicyclic transition state from a linear precursor, allowing only 1 of the 243 conformers of the CI to be open to SOZ formation. At this entropic limit, additional modes to store excess energy are irrelevant, as the rate-limiting issue is conformational. This is in contrast to the isomerization to vinyl hydroperoxide, which does not depend on the conformation of the carbon backbone. This reaction has a substantial barrier but a much higher entropy than the SOZ channel, so

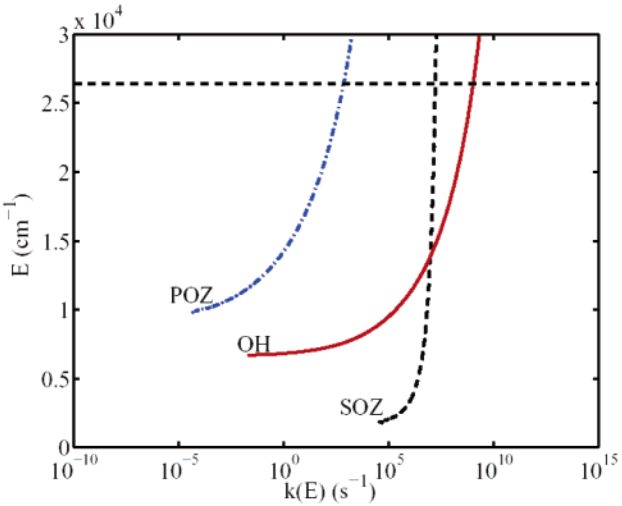

Figure 5. Microcanonical rate constants for the reaction pathways coming out of the syn-CI well (M5) in the O_3−cyclohexene reaction. Re-formation of the POZ (M4 via TS2, dash−dot blue line) is negligible. The two forward reactions compete. Formation of the SOZ (M6 via TS3, dashed black line) dominates at low energy, while formation of the vinyl hydroperoxide (M7 via TS4, solid red line), and ultimately OH radical, dominates at high energy. The crossover is well below the available energy (of ∼26 000 cm^{-1} and designated by the horizontal black dashed line), but well above the typical thermal energy, so the reaction mechanism should change with pressure as collisional stabilization occurs.

the microcanonical rate constant increases dramatically with energy above the barrier. In this case, extra vibrational modes store available energy effectively, and this energy is needed to promote the reaction; consequently, the microcanonical rate constants decrease substantially with increasing size.

The behavior of the rate constants for SOZ formation is worth a more detailed look. In particular, we shall address the low but constant (with carbon number) value of the high-energy regime, where entropy defines the rate constant. A naïve estimate of this entropic limit would be $k(E) = c\nu/243$ or $\sim 5 \times 10^{10}$ s^{-1} for $\nu = 500$ cm^{-1} (the factor of 243 is the number of CI conformers, only one of which leads to SOZ). However, the cycloaddition is even more constrained than this, as vibrations at the transition state are significantly stiffer than in the CI well. The microcanonical *A* factor ($k(\infty)$) is

$$A = c\left(\frac{\sigma_{TS}}{\sigma_r}\right)\left(\frac{I_r^3}{I_{TS}^3}\right)^{1/2} \nu_x \prod\left(\frac{\nu_r}{\nu_{TS}}\right) = c\nu_{eff} \qquad (6)$$

where σ_{TS} is the symmetry factor for the transition state, σ_r the symmetry factor for the reactant, I_r the moment of inertia of the reactant, I_{TS} the moment of inertia of the transition state, ν_x the frequency of the "extra" reactant mode corresponding to the reaction coordinate at the transition state (i.e., 500 cm^{-1} above), ν_r the frequencies of the reactant, ν_{TS} the corresponding frequencies of the transition state, and ν_{eff} the resulting effective frequency. The reactants have one more vibrational mode than the transition state (ν_x), but the full product of frequency ratios determines ν_{eff}. We can simply compare a sorted list of frequencies for the reactant (the CI) with a corresponding list of frequencies for the transition state; because of the ratio, only where there is a difference will there be a significant contribution to ν_{eff}. Also, the ratio of rotational moments may contribute, as will any symmetry factor (the number of channels). In this case, the moment of inertia contribution is minor, as most conforma-

Table 1. Calculation of the "Effective" Reaction Frequency for SOZ Formation from the Cyclohexene SCI

mode	ν(TS) (cm^{-1})	ν(CI) (cm^{-1})	ν(CI)/ν(TS)	cumulative product		ν_{eff} (cm^{-1})
"extra"		32	32			0.70
1	83	36	0.43			
2	190	95	0.50			
3	219	134	0.61			
4	255	165	0.65	(1−4)	0.085	
5	278	194	0.70			
6	349	234	0.67			
7	363	328	0.91			
8	433	335	0.77			
9	474	421	0.89	(5−9)	0.292	
10−50				(10−50)	0.883	

tions of the CI have similar moments, as does the TS. The symmetry factor is very important. It is effectively 1/243; while this is not true symmetry, it accounts for the many nonreactive conformations of the CI (with respect to SOZ formation).

There are significant changes between the CI and the TS for several frequencies because the CI has a succession of twisting modes with very low frequencies. These are really hindered internal rotations leading to conformational changes, but in addition they are simply very loose modes—the corresponding modes on the bicyclic transition state being much stiffer. Looking specifically at the computed frequencies, summarized in Table 1, we find the following: First, the "extra" mode on the reactant is the loosest, at only 32 cm^{-1}. Second, the next four modes average approximately one-half of the corresponding TS frequency, leading to a product of 0.085. Third, the next five modes are also rather looser than their analogues on the TS, further reducing the product of frequencies by 0.3. Finally, the remaining 40 modes, at 500 cm^{-1} and above, contribute only 0.9 in total to the product ratio. Combined, these factors conspire to produce an effective reaction frequency of less than 1 cm^{-1} (0.7 cm^{-1} to be exact). Consequently, the SOZ formation *A*-factor is approximately 1×10^8 s^{-1}, close to the value seen in Figure 5.

Overall, the major conclusions about the behavior of this system can be drawn from the microcanonical rate constants alone, without resorting to the master equation. In particular, the rate-limiting intermediate is the CI, as expected; any POZ stabilization at high pressure or carbon number will quickly lead to CI that would have been stabilized in any event—only at cryogenic temperatures will the POZ itself be of interest. In these endocyclic systems, the CI does indeed serve as a pressure switch, with vinyl hydroperoxide formation from chemically activated syn-CI (or dioxirane from anti-CI) and SOZ from SCI. The exact carbon number is unclear, but it is certainly greater than 6 at 1 atm pressure. However, there is an additional effect—with the added energy storage of extra nonreactive modes, the low-energy pathway becomes increasingly dominant, even at low pressure, as the system effectively self-thermalizes (with respect to branching). Consequently, at some carbon number (near 15), SOZ formation dominates at all pressures (though the SOZ will itself be chemically activated at low pressure, with unexplored consequences).

To be quantitative, we need to carry out master equation calculations. For our base case we shall assume an $\langle \Delta E \rangle_{down}$ of 500 cm^{-1} and use the microcanonical rate constants discussed above. The results are presented in Figures 6 and 7. Figure 6

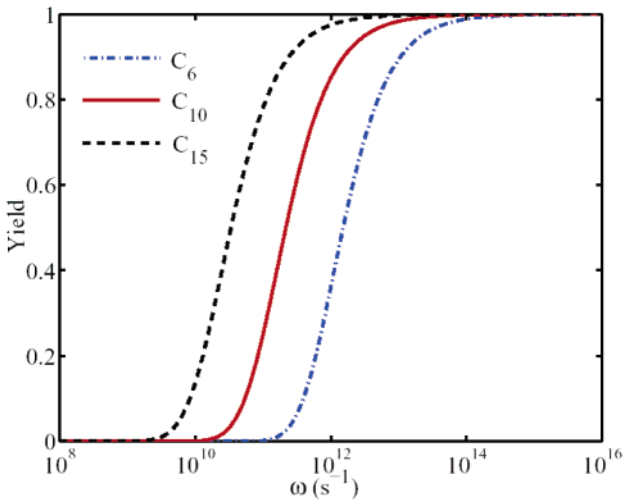

Figure 6. Yield of stabilized POZ (M4) from the ozonolysis of cyclohexene (C_6), 4,5-diethylcyclohexene (C_{10}), and 4-butyl-5-pentylcyclohexene (C_{15}). The center of the falloff curve ($\omega_{1/2}$) drops by one decade per five added carbons but remains above atmospheric pressure ($\sim 10^{10}$ Hz) for all systems. Stabilization of the POZ will occur at 1 atm for roughly ≥ C_{20} alkenes.

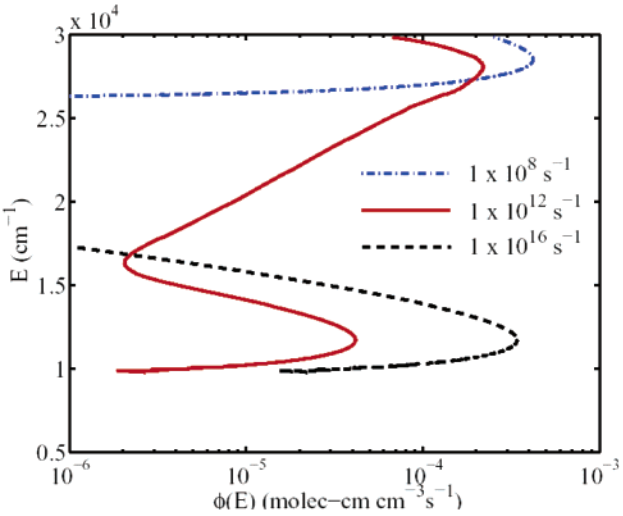

Figure 7. Flux distribution coming from the POZ well (M4) in the O_3−cyclohexene reaction from low to high collisional frequencies. Low frequency yields no stabilization and a flux essentially equal to the input flux. Intermediate pressure yields a bimodal distribution, while high pressure yields a single mode due to thermal decomposition of the stabilized POZ.

shows the yield of POZ as a function of collisional frequency from the ozonolysis of cyclohexene (C_6), 4,5-diethylcyclohexene (C_{10}), which can serve as a surrogate for monoterpenes, and 4-butyl-5-pentylcyclohexene (C_{15}), which can serve as an analogue for sesquiterpenes. This figure clearly shows that there is a dependence of collisional stabilization on size. As the carbon number increases, the collisional frequency for 50% yield decreases. For C_6, that is at 2×10^{12} s^{-1}; for C_{10}, 3×10^{11} s^{-1}; and for C_{15}, 5×10^{10} s^{-1}; consequently, for the POZ, the effect of added carbon atoms is, in rough terms, to increase the pressure by a factor of 10 for every 4−5 carbons added. The POZ itself should thus be collisionally stabilized at 1 atm pressure for a carbon number between 15 and 20 (regardless of the double bond location).

Figure 7 shows the flux distribution coming from the POZ well in the O_3−cyclohexene reaction as a function of energy at different collision frequencies (i.e., low, intermediate, and high

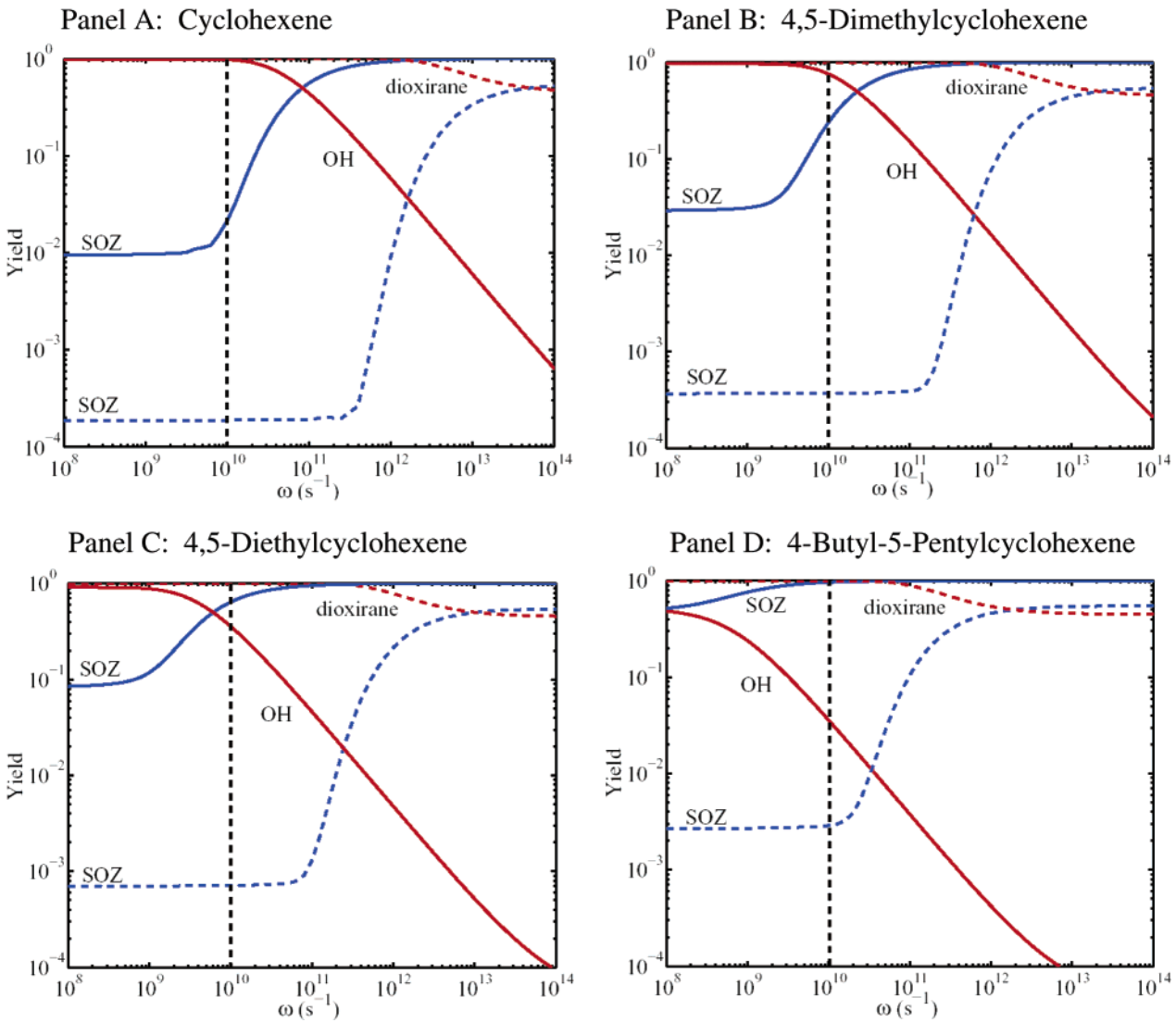

Figure 8. OH, dioxirane, and SOZ yields from the ozonolysis of cyclohexene (panel A), 4,5-dimethylcyclohexene (panel B), 4,5-diethylcyclohexene (panel C), and 4-butyl-5-pentylcyclohexene (panel D). Vertical dashed line is atmospheric pressure. Solid lines are yields from the syn pathway, and dashed lines are yields from the anti pathway. The crossover for syn and anti pathways is due to stabilization in the CI well, which results in SOZ formation being dominant. As carbon number increases (from panel A to panel D), the crossover in yields shifts to lower pressure for both syn and anti pathways.

Table 2. Low- and High-Pressure Limit OH, Dioxirane, and SOZ Yields from the Ozonolysis of Cyclohexene and Alkyl-Substituted Cyclohexenes

	OH yield		SOZ yield (from syn-CI)		dioxirane yield		SOZ yield (from anti-CI)	
compound	low-pressure limit	high-pressure limit	low-pressure limit	high-pressure limit	low-pressure limit	high-pressure limit	low-pressure limit	high-pressure limit
cyclohexene	0.99	4.4×10^{-5}	9.5×10^{-3}	0.99	0.99	0.45	1.9×10^{-4}	0.55
4,5-dimethylcyclohexene	0.97	4.5×10^{-5}	3.0×10^{-2}	0.99	0.99	0.45	3.7×10^{-4}	0.55
4,5-diethylcyclohexene	0.92	4.6×10^{-5}	8.2×10^{-2}	0.99	0.99	0.45	7.0×10^{-4}	0.55
4-butyl-5-pentylcyclohexene	0.53	4.7×10^{-5}	0.47	0.99	0.99	0.45	2.7×10^{-3}	0.55

pressures). The flux distribution is bimodal. The high-energy, low-pressure mode is interesting, as it may either be collisionally stabilized or continue to form vinyl hydroperoxide and thus OH. The low-energy mode will certainly be stabilized. It is interesting to note that the maximum energy of the high-energy mode decreases slightly with increasing energy; as a consequence, the pressure falloff curves will be sharper than the classical Lindemann−Hinshelwood curve, as the mean intermediate lifetime will increase with increasing pressure. The bimodal flux distribution is also observed for C_8-C_{15} alkyl-substituted cyclohexenes.

The yields of OH, dioxirane, and SOZ from the ozonolysis of cyclohexene and the C_8-C_{15} alkyl-substituted cyclohexenes (both anti and syn pathways) as a function of collisional frequency are shown in Figure 8. The panels in this figure clearly show that the OH, dioxirane, and SOZ yields have low- and high-pressure limits, which are shown in Table 2. At atmospheric pressure, the OH yield is essentially unity for the cyclohexene case, and this is also the low-pressure limit. This is expected, as the syn pathway is efficient at producing OH. Given that the syn/anti branching ratio is ~60/40 and that OH production from the anti pathway is ~5−15%, the total OH

yield from cyclohexene ozonolysis would be ~0.62−0.68, which agrees with the experimental values of 0.54 ± 0.13 and $0.68^{+0.34}_{-0.22}$.[56]

Figure 8 reveals the features suggested by the microcanonical rate constants. The center of the stabilization falloff curves (where the OH channel is reduced by a factor of 2) moves from 9×10^{10} s^{-1} for cyclohexene to 3×10^{10}, 8×10^{9}, and 8×10^{7} s^{-1} for the C_8, C_{10}, and C_{15} compounds, respectively. Concurrently, the low-pressure limit for SOZ formation rises progressively, from approximately 1% for cyclohexene to 50% for the C_{15} compound. The exact pressures and carbon numbers depend on relatively uncertain parameters, such as $\langle \Delta E \rangle_{down}$ and the barrier heights for the competing processes (see Supporting Information), but the overall conclusions do not change: collisional stabilization occurs first with the CI, and at atmospheric pressure the stabilization becomes dominant for some carbon number between 8 and 15—in atmospheric terms, between something slightly smaller than monoterpenes and sesquiterpenes. The SCI has an exceedingly short lifetime (~70 ns) against isomerization to SOZ, which is thus expected to be the dominant initial product for the larger, endocyclic alkenes. A sensitivity analysis to these uncertain parameters is presented in the Supporting Information. With the exception of the cyclohexene case, the SOZ product will have a very low vapor pressure and will thus partition efficiently into the aerosol phase. A single-product model should adequately describe aerosol yields for these species.[47]

There are differences between the syn and anti pathways, as shown in Figure 8. These are caused by a lower barrier for dioxirane formation than for vinyl hydroperoxide formation in the syn pathway (13.3 kcal mol^{-1}, instead of 19.1 kcal mol^{-1}, a 5.8 kcal mol^{-1} difference). Consequently, the intermediate is more difficult to stabilize and the dioxirane pathway is generally more favorable. Even at the high-pressure limit, SOZ and dioxirane yields from the anti pathway are 55 and 45%, respectively, for cyclohexene and the other compounds, as shown in Figure 8. Stabilization is again progressively easier with increasing carbon number, with the center of the stabilization falloff curves (where the dioxirane channel is reduced by a factor of 2) moving from 7×10^{13} s^{-1} for cyclohexene to 3×10^{13}, 8×10^{12}, and 2×10^{12} s^{-1} for the C_8, C_{10}, and C_{15} compounds, respectively. However, even the C_{15} sesquiterpene analogue is not stabilized at 1 atm.

The differences between the syn and anti pathways should be regarded, in the main, as a measure of the uncertainty in this system. The relatively low level of theory used here is but a small part of those uncertainties; collisional energy transfer is another, our assumption that statistical reaction dynamics are accurate is a third, and the incredible complexity of the complete potential energy surface is a fourth. Only with careful experimental study of these systems will more accurate computational efforts be warranted, or will their interpretation be possible.

Our results are broadly consistent with the available experimental evidence on endocyclic alkenes. In particular, OH yields are generally high for species up to monoterpenes, with yields depending primarily on the degree of substitution around the double bond, and thus presumably governed by the branching between syn and anti isomers of the CI (not within the scope of this study).[32,33,56−58] The sesquiterpenes, however, show a very high yield of condensable products and essentially no behavior consistent with stabilized radicals, such as a dependence on water.[59] The reduced OH yields are consistent with stabilization, but the absence of scavenging effects is consistent with unimolecular sequestration of the intermediates, such as with the SOZ formation suggested here. This is consistent with the findings of Hatakeyama et al.,[26] who observed decreasing H_2SO_4 yields with increasing size of simple endocyclic alkenes and attributed this observation to stabilization of the CI and the ensuing intramolecular reaction to form SOZ. The behavior of diolefinic terpenes is likely to be more complicated, as these typically contain at least one endo- and one exocyclic double bond. Combining experimental and computational evidence, it is likely that the transition from chemically activated to collisionally stabilized processes for endocyclic alkenes at atmospheric pressure occurs between C_{10} (monoterpenes) and C_{15} (sesquiterpenes).

Conclusions

The fate of the primary ozonide and Criegee intermediates from the ozonolysis of cyclohexene and alkyl-substituted cyclohexenes has been determined using RRKM/master equation calculations, though the broad conclusions could be drawn from the microcanonical rate constants alone. For all of the systems considered here, the primary ozonide (POZ) decomposes rapidly, giving a mixture of vibrationally excited syn and anti Criegee intermediates containing essentially all of the available reaction energy. POZ stabilization will occur at a carbon number near 20. Vibrationally excited syn-CI from the O_3−cyclohexene reaction produces vinyl hydroperoxide with essentially unit yield. This will lead to OH production. Because of the very different barriers to the two competing pathways (OH and SOZ), the branching ratio changes with increasing carbon number, progressively favoring SOZ formation. At the largest carbon numbers, SOZ formation competes with OH formation even at low pressure. Because the total rate constant at high energies out of the CI well is lower than that out of the POZ well, it is expected that collisional stabilization will occur first in the CI well, then in the POZ. Any stabilized POZ will lead to the production of SCI and eventual SOZ formation.

The microcanonical rate constants also reveal that the formation of SOZ is dominated by entropy because of the constraint of forming a bicyclic transition state from a linear precursor. The rate-limiting issue is now conformational, as extra vibrational modes do not affect the microcanonical rate constants. This is in contrast to the isomerization pathway to form a vinyl hydroperoxide, which does not depend on the conformation of the CI, as the extra vibrational modes store energy effectively, causing the microcanonical rate constants to decrease with increasing carbon number and favoring the SOZ formation. It appears that in these endocyclic systems, the CI essentially serves as a pressure switch with vinyl hydroperoxide or dioxirane formation occurring from chemically activated syn-CI and SOZ formation occurring from collisionally stabilized

(56) Calvert, J. G.; Atkinson, R.; Kerr, J. A.; Madronich, S.; Moortgat, G. K.; Wallington, T. J.; Yarwood, G. *The Mechanisms of Atmospheric Oxidation of Alkenes*; Oxford University Press: New York, 2000.
(57) Atkinson, R. *J. Phys. Chem. Ref. Data* **1997**, *26*, 215.
(58) Atkinson, R. *Atmos. Environ.* **2000**, *34*, 2063.
(59) Bonn, B.; Moortgat, G. K. *Geophys. Res. Lett.* **2003**, *30*, 1585.
(60) Treacy, J.; Curley, M.; Wenger, J.; Sidebottom, H. *J. Chem. Soc., Faraday Trans.* **1997**, *93*, 2877.

syn-CI. It is at some carbon number between 8 and 15 (or between something slightly smaller than monoterpenes and sesquiterpenes) that SOZ formation dominates at all pressures.

The conclusions drawn from the microcanonical rate constants are confirmed by the results of the master equation calculations. A dependence of collisional stabilization on size is observed for both the POZ and the CI. As carbon number is increased, the collisional frequency for 50% yield of stabilized POZ and SCI decreases. In the case of the POZ, the effect of increasing carbon number is essentially to increase the pressure by a factor of 10 for every 4−5 carbons added. In the case of the CI, the centers of the OH and dioxirane yield falloff curves decrease while the low-pressure limit for SOZ formation increases with increasing carbon number. Indeed, the CI serves as a pressure switch.

Given the result that SOZ formation dominates at atmospheric pressure in the ozonolysis of the sesquiterpene analogue, it is not expected that one would be able to measure any ambient SCI from endocyclic sesquiterpene ozonolysis because we expect that any SCI formed would quickly cyclize to form SOZ. Indeed, the ozonolysis of sesquiterpenes is very efficient at producing SOZ, and thus efficient at producing secondary organic aerosol. Furthermore, we do not expect SCI from endocyclic sesquiterpene ozonolysis to undergo bimolecular reaction (including that with H_2O, as implied by Bonn and Moortgat[59]) since its lifetime is too short (∼70 ns) compared to the rate of bimolecular reaction.

Acknowledgment. This work is supported by grant ATM0125283 from the National Science Foundation.

Supporting Information Available: Sensitivity of results to barrier heights and $\langle \Delta E \rangle_{\text{down}}$, uncertainty in barrier heights, single-point QCISD(T) calculations of smaller analogous Criegee intermediates, optimized geometries, energies, and frequencies. This material is available free of charge via the Internet at http://pubs.acs.org.

JA0485412